F-Loss and H-Loss Dissociations in Low-Lying Electronic States of the CH_3F^+ Ion Studied Using Multiconfiguration Second-Order Perturbation Theory

Hong-Wei Xi, Ming-Bao Huang,* Bo-Zhen Chen, and Wen-Zuo Li

College of Chemistry and Chemical Engineering, Graduate School, Chinese Academy of Sciences, P.O. Box 4588, Beijing 100049, People's Republic of China

Received: May 12, 2005; In Final Form: August 6, 2005

Complete active space self-consistent field (CASSCF) and multiconfiguration second-order perturbation theory (CASPT2) calculations with an atomic natural orbital basis were performed for the $1^2A''$, $1^2A'$, $2^2A'$, $2^2A''$, and $3^2A'$ (X^2E, A^2A_1, and B^2E) states of the CH_3F^+ ion. The $1^2A''$ state is predicted to be the ground state, and the C_s-state energy levels are different from those of the CH_3Cl^+ ion. The $2^2A'$ (A^2A_1) state is predicted to be repulsive, and the calculated adiabatic excitation energies for $2^2A''$ and $3^2A'$ are very close to the experimental value for the B state. The CASPT2//CASSCF potential energy curves (PECs) were calculated for F-loss dissociation from the five C_s states and H-loss dissociation from the $1^2A''$, $1^2A'$, and $2^2A''$ states. The electronic states of the CH_3^+ and CH_2F^+ ions as the dissociation products were carefully determined by checking the energies and geometries of the asymptote products, and appearance potentials for the two ions in different states are predicted. The F-loss PEC calculations for CH_3F^+ indicate that F-loss dissociation occurs from the $1^2A''$, $1^2A'$, and $2^2A'$ states [all correlating with $CH_3^+(X^1A_1')$], which supports the experimental observations of direct dissociation from the X and A states, and that direct F-loss dissociation can occur from the two Jahn−Teller component states of B^2E, $2^2A''$ and $3^2A'$ [correlating with $CH_3^+(1^3A'')$ and $CH_3^+(1^3A')$, respectively]. Some aspects of the $3^2A'$ Cl-loss PEC of the CH_3Cl^+ ion are inferred on the basis of the calculation results for CH_3F^+. The H-loss PEC calculations for CH_3F^+ indicate that H-loss dissociation occurs from the $1^2A''$, $1^2A'$, and $2^2A''$ states [correlating with $CH_2F^+(1^3A'')$, $CH_2F^+(X^1A_1)$, and $CH_2F^+(1^1A'')$, respectively], which supports the observations of direct dissociation from the X and B states. As the $2^2A'$ H-loss PEC of CH_3Cl^+, the $2^2A'$ H-loss PEC of CH_3F^+ does not lead to $H + CH_2X^+$, but the PECs of the two ions represent different types of reactions.

I. Introduction

During the past three decades, numerous experimental studies[1−8] on dissociation of the fluoromethane ion (CH_3F^+) from its low-lying electronic states have been reported. Since the electron configuration of the ground-state CH_3F molecule is $...(3a_1)^2(4a_1)^2(1e)^4(5a_1)^2(2e)^4$ (in the C_{3v} symmetry), the X^2E $[(2e)^{-1}]$, A^2A_1 $[(5a_1)^{-1}]$, and B^2E $[(1e)^{-1}]$ states were considered to be the three lowest-lying electronic states of the CH_3F^+ ion in those previous experimental studies. In 1976 Eland et al.[1] presented a general picture for dissociation of the CH_3F^+ ion from the X, A, and B states (see the scheme of the fragmentation pathways in ref 1), based on their photoelectron−photoion coincidence (PEPICO) experiments. They observed direct F-loss dissociation from the X and A states to CH_3^+ and direct H-loss dissociation from the X and B states to CH_2F^+. They did not observe H-loss dissociation from the A state, and they proposed F-loss dissociation from the B state via internal conversion from B to A. Several later experimental studies (by Locht and coworkers[2−6] and Olney et al.[7]) supported the general picture of Eland et al. and measured appearance potentials (APs) for the CH_3^+ and CH_2F^+ ions.

In the general picture of Eland et al.,[1] the Jahn−Teller splitting in the E states (X and B) was not explicitly considered. The degeneracy of a ^2E state is removed by a Jahn−Teller distortion of the geometry from C_{3v} to C_s symmetry giving rise to one $^2A'$ and one $^2A''$ state. Hence, the three C_{3v} states (X^2E, A^2A_1, and B^2E) of the CH_3F^+ ion become five C_s states: $1^2A''$, $1^2A'$, $2^2A'$, $2^2A''$, and $3^2A'$ (the electron configuration of the ground-state CH_3F molecule becoming $...(3a')^2(4a')^2(5a')^2(1a'')^2(6a')^2(7a')^2(^2a'')^2$ in the C_s symmetry). Therefore, in theoretical studies on F-loss and H-loss dissociation of the CH_3F^+ ion, one should explicitly consider the C_s states, and one should also explicitly give electronic states of the CH_3^+ and CH_2F^+ ions as dissociation products from different C_s states.

To the best of our knowledge, there is no reported theoretical study on F-loss or H-loss dissociation of the CH_3F^+ ion from these electronic states in the literature. It is known that the CASSCF (complete active space self-consistent field)[9] and CASPT2 (multiconfiguration second-order perturbation theory)[10,11] methods are effective for theoretical studies of excited electronic states of molecules and molecular ions. By using the CASSCF and CASPT2 methods, we previously studied Cl-loss dissociation of the CH_3Cl^+ ion from the $1^2A'$, $1^2A''$, $2^2A'$, and $2^2A''$ states (the X^2E, A^2A_1, and B^2E states of CH_3Cl^+ becoming $1^2A'$, $1^2A''$, $2^2A'$, $3^2A'$, and $2^2A''$) and H-loss dissociation from the $1^2A'$, $1^2A''$, and $2^2A''$ states.[12] The purpose of the present work is to study F-loss and H-loss dissociation of the CH_3F^+ ion from the $1^2A''$, $1^2A'$, $2^2A'$, $2^2A''$, and $3^2A'$ states using the CASSCF and CASPT2 methods. Before we calculated dissociation reaction paths, we calculated geometries and energetics for the five C_s states of the CH_3F^+ ion using these methods. The geometries and energetics of the $1^2A''$ and $1^2A'$ states of CH_3F^+

* Corresponding author. E-mail: mbhuang1@gscas.ac.cn.

10.1021/jp0524835 CCC: $30.25
Published on Web 09/16/2005

TABLE 1: CASSCF-Optimized Geometries for the $1^2A''$, $1^2A'$, $2^2A'$, $2^2A''$, and $3^2A'$ States of the CH_3F^+ Ion[a,b]

state	R(C−F) (Å)	R(C−H_1) (Å)	R(C−H_2) (Å)	A(H_1CF) (deg)	A(H_2CF) (deg)	D(H_2CFH_2') (deg)	imaginary frequency (cm^{-1})[c]
$1^2A''$(X^2A'')	1.280	1.096	1.170	118.1	112.4	142.0	no
	(1.274)[d]	(1.084)	(1.172)	(118.0)	(110.8)		no
$1^2A'$	1.301	1.237	1.096	99.2	114.7	103.3	−586.9
	(1.286)[d]	(1.233)	(1.100)	(104.7)	(116.6)		(−827.6)[d]
$2^2A'$ [e]							
$2^2A''$	1.623	1.073	1.146	105.1	107.2	100.8	no
$3^2A'$	1.617	1.190	1.086	106.5	106.5	110.7	−632.2

[a] Bond length, bond angle, and dihedral angle are denoted as R, A, and D, respectively; for notations, see Figure 1. [b] $1^2A''$ and $1^2A'$ are the two Jahn−Teller component states of X^2E, and $2^2A''$ and $3^2A'$ are the two Jahn−Teller component states of B^2E. [c] Unique imaginary frequencies were obtained for $1^2A'$ and $3^2A'$ in the CASSCF frequency calculations, and they are associated with H-pivotal rotations. [d] Values in parentheses are the MP2 geometric parameters and the imaginary frequency from ref 14. [e] $2^2A'$ is predicted to be a repulsive state.

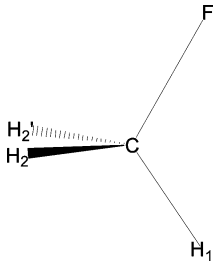

Figure 1. Atom labelings in the fluoromethane ion used in the present study.

were previously calculated by Locht et al.,[13] Mahapatra et al.,[14] and Gauld et al.[15] using the MP2 method. In the present article we will first briefly report the calculated geometries and energetics for the five C_s states and then present a detailed description of the calculated reaction paths for F-loss and H-loss dissociation from these C_s states. In the conclusion section of the present article, we will comment on the general picture of Eland et al.[1] on the basis of our predicted dissociation mechanisms for the CH_3F^+ ion, and we will compare the calculation results for the CH_3F^+ ion with those for the CH_3Cl^+ ion.[12]

II. Calculational Details

The geometry and atom labeling used for the CH_3F^+ ion (C_s symmetry) are shown in Figure 1. The H_1 atom in the symmetry plane is assumed to be the leaving species in H-loss dissociation. The CAS (CASSCF and CASPT2) calculations were carried out using the MOLCAS v5.4 quantum-chemistry software.[16] With a CASSCF wave function constituting the reference function, the CASPT2 calculations were performed to compute the first-order wave function and the second-order energy in the full-CI space. A contracted atomic natural orbital (ANO) basis set,[17−19] F[6s4p3d1f], C[5s3p2d1f], and H[3s2p1d], were used. The CASSCF geometry optimization and frequency calculations were performed for the five C_s states ($2^2A'$ being predicted to be repulsive). On the basis of the CASPT2 calculations at the CASSCF-optimized geometries, we obtained the CASPT2//CASSCF adiabatic excitation energies (T_0's) ($1^2A''$ being predicted to be the ground state). Based on the CASPT2 calculations at the CASSCF geometry of the $1^2A''$ state, we obtained the CASPT2//CASSCF vertical excitation energies (T_v's). On the basis of the CASPT2 calculations for the five C_s states at the experimental geometry[20] of the ground-state CH_3F molecule (abbreviated to "experimental molecular geometry"), we obtained the CASPT2 relative energies (denoted as T_v''s) of the five C_s states (to $1^2A''$).

For F-loss dissociation from the five C_s states of CH_3F^+, the C−F distance [R(C−F)] was taken as the reaction coordinate. At a set of fixed R(C−F) values ranging from the C−F bond length values in the CASSCF-optimized geometries of the respective states (except $2^2A'$) to 4.0 Å, we performed the CASSCF partial geometry optimization calculations and the CASPT2 energy calculations at the five sets of the partially optimized geometries, and we obtained the CASPT2//CASSCF potential energy curves (PECs) for F-loss dissociation from the five C_s states. For H-loss dissociation the C−H_1 distance [R(C−H_1)] was taken as the reaction coordinate. At a set of fixed R(C−H_1) values ranging from the C−H_1 bond length values in the CASSCF optimized geometries to 4.0 Å, we performed the CASSCF partial geometry optimization calculations and the CASPT2 energy calculations, and we obtained the CASPT2// CASSCF PECs for H-loss dissociation from the $1^2A'$, $1^2A''$, and $2^2A''$ states. We failed to calculate H-loss PEC for $3^2A'$ because of converge problems in CASSCF partial geometry optimization calculations. In the H-loss PEC calculations for $2^2A'$, the H^+ ion was predicted to be the dissociation product (see section III.C.).

In the CASSCF calculations, we used the full-valence active space, which includes eight a′ (6a′−13a′) and three a″ (2a″−4a″) orbitals (13 electrons and 11 active orbitals). In the CASPT2 calculations, the weight values of the CASSCF reference functions in the first-order wave functions were all larger than 0.8542. In the CASSCF geometry optimization and CASPT2//CASSCF energetic calculations for low-lying electronic states of the dissociation products, CH_3^+ and CH_2F^+, the full-valence active spaces were used.

III. Results and Discussion

III.A. Geometries and Excitation Energies. The $2^2A'$ state is predicted to be repulsive about the C−F bond in the CASSCF geometry optimization calculations. In Table 1 are given the CASSCF-optimized geometries for the $1^2A''$, $1^2A'$, $2^2A''$, and $3^2A'$ states. The CASSCF frequency calculations predict that the $1^2A'$ and $3^2A'$ states have unique imaginary frequencies (see Table 1). The vibration modes associated with these imaginary frequencies describe pivotal motion of the three hydrogen atoms, and therefore these imaginary frequencies are not related to transition states (if any) in F-loss or H-loss dissociation reactions of the $1^2A'$ and $3^2A'$ states. In Table 2 are given the CASPT2// CASSCF T_0 values for the $1^2A''$, $1^2A'$, $2^2A''$, and $3^2A'$ states and the CASPT2//CASSCF T_v values and CASPT2 T_v' values for the $1^2A''$, $1^2A'$, $2^2A'$, $2^2A''$, and $3^2A'$ states. The CASPT2// CASSCF T_0 and T_v results indicate that $1^2A''$ is the ground state of the CH_3F^+ ion. Based on their photoelectron spectrum, Karlsson et al.[21] reported an adiabatic ionization potential (AIP) value of 12.533 eV and a vertical ionization potential (VIP) value of 13.038 eV for the X^2E state of CH_3F^+. Karlsson et al.[21] found that peaks for the A^2A_1 and B^2E states of CH_3F^+ on spectrum entirely overlapped, and they reported the same AIP

TABLE 2: CASPT2 Adiabatic (T_0) and Vertical (T_v) Excitation Energies for the $1^2A''$, $1^2A'$, $2^2A'$, $2^2A''$, and $3^2A'$ States of the CH_3F^+ Ion Calculated Using the CASSCF-Optimized Geometries and the CASPT2 Relative Energies (T_v') of the Five States Calculated at the Experimental Geometry of the Ground-State CH_3F Molecule[a]

	T_0 (eV)		T_v (eV)	T_v' (eV)	
state	calcd	exptl[b]	calcd	calcd	exptl[c]
$1^2A''(X^2A'')$	0.00	X^2E: 0.00	0.00	0.00	X^2E: 0.00
$1^2A'$	0.11		2.87	0.01	
$2^2A'$	d	A^2A_1: 3.77	7.08	3.97[e]	A^2A_1: 4.16
$2^2A''$	3.67	B^2E: 3.77	6.12	3.90	B^2E: 4.16
$3^2A'$	3.71		7.64	3.93[e]	

[a] From ref 20, the experimental geometry: R(C−F) = 1.383 Å, R(C−H) = 1.087 Å, A(HCF) = 108.7°, and D(HCFH) = 120.0°. [b] Evaluated using the experimental AIP data reported in ref 21 (the AIP value for X^2E is 12.533 eV). [c] Evaluated using the experimental VIP data reported in ref 21 (the VIP value for X^2E is 13.038 eV). [d] A is a repulsive state. [e] In the CASSCF calculations, $2^2A'$ (the second root) had a lower energy than $3^2A'$ (the third root).

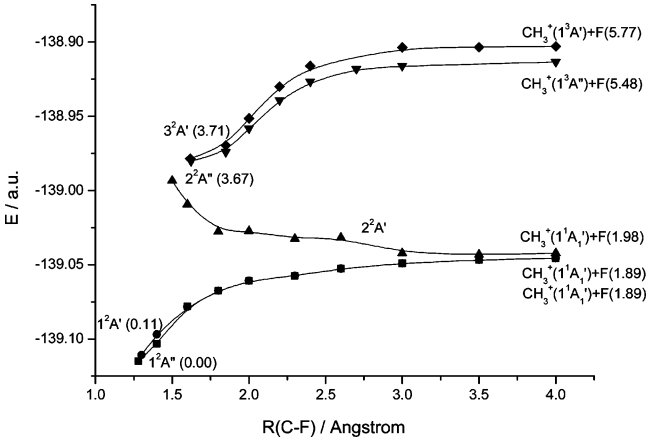

Figure 2. CASPT2//CASSCF potential energy curves for F-loss dissociation from the $1^2A''$, $1^2A'$, $2^2A'$, $2^2A''$, and $3^2A'$ states. In parentheses are given the CASPT2//CASSCF relative energies (in eV) of the asymptote products to the $1^2A''$ reactant.

value of 16.3 eV and the same VIP value of 17.2 eV for the A and B states. The T_0 values for the CH_3F^+ ion are considered to be equal to the differences between the AIP values for excited states and the AIP value for the ground state, and therefore, the experimental T_0 values are 3.767 eV for A^2A_1 and B^2E. The T_v' values for the CH_3F^+ ion are considered to be equal to the differences between the VIP values for excited states and the VIP value for the ground state, and therefore, the experimental T_v' values are 4.162 eV for A^2A_1 and B^2E. All these experimental T_0 and T_v' values, evaluated using the experimental AIP and VIP values,[21] are listed in Table 2.

The CASSCF geometries for the $1^2A''$ and $1^2A'$ states (the two Jahn−Teller component states of X^2E) are notably different. The C−H_1 bond length (1.237 Å) in the $1^2A'$ geometry is significantly longer than that in the $1^2A''$ geometry, while the H_2CFH_2' dihedral angle (142.0°) in the $1^2A''$ geometry is much larger than that in the $1^2A'$ geometry. Three groups[13−15] previously studied the $1^2A''$ and $1^2A'$ states of CH_3F^+ using the MP2 method. Listed in Table 1 are the MP2 geometric parameters and unique imaginary frequency (for $1^2A'$) predicted by the latest MP2 study,[14] which are similar to our CASSCF results for these two states. The CASSCF geometries for the $2^2A''$ and $3^2A'$ states (the two Jahn−Teller component states of B^2E) are also notably different. The C−H_1 bond length (1.190 Å) in the $3^2A'$ geometry is significantly longer than that in the $2^2A''$geometry, while the H_2CFH_2' dihedral angle in the $2^2A''$ geometry is smaller than that in the $3^2A'$ geometry. The C−F bond lengths in both the $2^2A''$ and $3^2A'$ geometries are longer than 1.6 Å.

We report no CASPT2//CASSCF T_0 value for the repulsive $2^2A'$ state, though the experimental AIP for A^2A_1 was reported[21] and the evaluated experimental T_0 value of 3.77 eV is listed in Table 2. On the basis of the CASPT2//CASSCF T_0 results given in Table 2, we realize the Jahn−Teller splitting pattern in the X^2E ($1^2A' + 1^2A''$) and B^2E ($3^2A' + 2^2A''$) states of the CH_3F^+ ion: the A′ components are higher in energy (T_0) than the respective A″ components. Our previous CASPT2//CASSCF study for the CH_3Cl^+ ion[12] predicted a different Jahn−Teller splitting pattern in the X^2E state: the A″ component is higher in energy (T_0) than the A′ component (the $^2A''$ state having unique imaginary frequency). The CASPT2//CASSCF T_0 values for $2^2A''$ and $3^2A'$ (3.67 and 3.71 eV, respectively) are very close to the experimental T_0 value of 3.77 eV for the B^2E state.[21]

The small CASPT2 T_v' value (0.01 eV) for $1^2A'$ indicates that the $1^2A'$ and X^2A'' states are close-lying at the experimental molecular geometry. The close CASPT2 T_v' values for $2^2A'$, $2^2A''$, and $3^2A'$ indicate that the three states are close-lying at the experimental molecular geometry, in line with the experimental fact[21] that peaks for the A^2A_1 and B^2E states of CH_3F^+ on spectrum entirely overlapped and the A and B states have the same VIP value. The CASPT2 T_v' values for the $2^2A'$, $2^2A''$, and $3^2A'$ states (3.97, 3.90, and 3.93 eV, respectively) are 0.19−0.26 eV smaller than the experimental T_v' value of 4.16 eV for the A and B states, and the agreements are reasonably good (for the calculated T_v' values for $2^2A'$ and $3^2A'$, see footnote *e* for Table 2).

There are no available experimental T_v data. Compared to the T_0 and T_v' values, the calculated T_v values are large, which indicates that the four excited states are high-lying at the X^2A'' geometry. It is noted that the $2^2A'$ state lies between $2^2A''$ and $3^2A'$ at the X^2A'' geometry.

III.B. F-Loss Dissociation. In Figure 2 are given the CASPT2//CASSCF PECs for F-loss dissociation from the $1^2A''$, $1^2A'$, $2^2A'$, $2^2A''$, and $3^2A'$ states [abbreviated to "$1^2A''$ (F-loss) PEC, ..."] of the CH_3F^+ ion. The CH_3F^+ systems in the five states at the R(C−F) value of 4.0 Å will be called F-loss dissociation asymptote products of the five states [abbreviated to "$1^2A''$ (F-loss) asymptote product, ..."] in the present section. We will use similar abbreviations for the PECs and asymptote products for H-loss dissociation in section III.C. The CASPT2//CASSCF relative energies of the asymptote products of the five states to the $1^2A''$ reactant (the $1^2A''$ state at the CASSCF equilibrium geometry) are given in parentheses in Figure 2. In Table 3 are listed the CASPT2//CASSCF energies of the five states at selected R(C−F) values, together with charges on the F atom [Q(F)] and values of principal geometric parameters in the CASSCF partially optimized geometries.

As shown in Table 3, the Q(F) values in the asymptote products of the five states are all very small (−0.001 or 0.000 *e*), which indicates that the products of F-loss dissociation from the five states are the neutral F atom plus the CH_3^+ ion in different states. In Table 4 given are the CASSCF geometries and CASPT2//CASSCF relative energies (T_0's) for the $1^1A'$ ($1^1A_1'$), $1^3A''$, and $1^3A'$ states (the three lowest-lying states) of the CH_3^+ ion. The $1^2A''$, $1^2A'$, and $2^2A'$ asymptote products have similar CASPT2//CASSCF energies (see Table 3), and the geometries of the CH_3 fragment in the asymptote products of the three states are almost identical to the CASSCF geometry of the $1^1A_1'$ state of the CH_3^+ ion (see Tables 3 and 4). We

TABLE 3: CASPT2//CASSCF Energies (*E*'s) at the Selected *R*(C−F) Values for F-Loss Dissociation from the $1^2A''$, $1^2A'$, $2^2A'$, $2^2A''$, and $3^2A'$ States, Together with Charge Values (*Q*'s) on the F Atom and Values of Principal Geometric Parameters in the CASSCF Partially Optimized Geometries[a]

R(C−F) (Å)	*E* (au)	*Q*(F) (*e*)	*R*(C−H$_2$) (Å)	*A*-(H$_2$CH$_2'$) (deg)	*D*-(H$_2$CH$_1$H$_2'$) (deg)	*R*-(C−H$_1$) (Å)
			$1^2A''$			
1.280	−139.11499	0.102	1.170	69.5	80.1	
1.4	−139.10325	−0.001	1.162	72.6	87.6	
1.6	−139.07809	0.322	1.104	114.3	145.7	
1.8	−139.06762	0.237	1.097	117.9	157.7	
2.0	−139.06081	0.148	1.096	119.1	166.9	
2.3	−139.05742	0.059	1.097	119.8	175.5	
3.0	−139.04901	0.004	1.099	120.0	179.5	
4.0	−139.04564	−0.001	1.099	120.0	179.9	
			$1^2A'$			
1.301	−139.11086	0.132	1.096	124.4	126.6	
1.4	−139.09686	−0.002	1.083	127.5	130.3	
1.6	−139.07838	0.321	1.097	119.7	147.2	
1.8	−139.06762	0.237	1.096	119.6	158.2	
2.0	−139.06084	0.147	1.096	120.0	167.1	
2.3	−139.05741	0.058	1.097	120.3	175.5	
3.0	−139.04899	0.004	1.099	120.1	179.6	
4.0	−139.04564	−0.001	1.099	120.1	179.8	
			$2^2A'$			
1.4	−138.96975	0.322	1.107	116.9	145.5	
1.6	−139.00928	0.206	1.100	118.8	158.7	
1.8	−139.02761	0.131	1.098	119.8	168.6	
2.0	−139.02719	0.070	1.100	119.8	172.6	
2.3	−139.03241	0.032	1.085	121.0	179.2	
2.6	−139.03177	0.011	1.080	120.3	179.8	
3.0	−139.04226	0.002	1.097	120.1	179.8	
4.0	−139.04226	0.000	1.102	121.2	179.7	
			$2^2A''$			
1.623	−138.98015	0.073	1.146	94.8	117.9	
1.85	−138.97415	−0.010	1.182	79.2	104.6	
2.0	−138.95822	−0.012	1.185	73.6	98.5	
2.2	−138.93924	0.000	1.187	67.8	89.8	
2.4	−138.92671	0.007	1.188	64.3	83.7	
2.7	−138.91810	0.007	1.188	62.2	79.7	
3.0	−138.91617	0.005	1.188	61.8	78.5	
4.0[b]	−138.91349	−0.001	1.188	61.8	78.5	
			$3^2A'$			
1.617	−138.97861	0.061	1.096	127.5	135.3	1.190
1.85	−138.96967	−0.021	1.110	136.1	138.9	1.293
2.0	−138.95146	−0.028	1.111	138.7	140.1	1.311
2.2	−138.93010	−0.013	1.111	139.6	140.3	1.320
2.4	−138.91620	0.001	1.112	139.5	139.8	1.314
3.0	−138.90371	0.005	1.113	138.1	138.2	1.301
4.0	−138.90297	−0.001	1.113	138.5	138.6	1.303

[a] For notations, see Figure 1. [b] All the other geometrical parameters were fixed at the values in the partially optimized geometry at *R*(C−F) = 3.0 Å.

TABLE 4: CASSCF Geometries and CASPT2//CASSCF Relative Energies (T_0's) for the $1^1A'$, $1^3A''$, and $1^3A'$ States (the Three Lowest-Lying States) of the CH_3^+ Ion[a]

state	*R*(C−H$_1$) (Å)	*R*(C−H$_2$) (Å)	*A*(H$_2$CH$_2'$) (deg)	*D*(H$_2$CH$_1$H$_2'$) (deg)	T_0 (eV)
$1^1A_1'$ [b]	1.097	1.100	119.8	180.0	0.0
$1^3A''$	1.096	1.196	56.0	68.2	3.56
$1^3A'$	1.302	1.114	138.5	138.6	3.86

[a] For notations, see Figure 1. [b] The $1^1A_1'$ (D_{3h}) state was calculated as $1^1A'$ within the C_s symmetry, and the calculations did not produce the exact *A*(H$_2$CH$_2'$) value of 120°.

conclude that the $1^2A''$, $1^2A'$, and $2^2A'$ states of the CH_3F^+ ion all correlate with the $1^1A_1'$ ground state of the CH_3^+ ion. As shown in Figure 2, the $1^2A''$ and $1^2A'$ F-loss PECs almost coincide.

In the CASPT2//CASSCF calculations for the $2^2A''$ F-loss PEC, we had convergence problems in the CASSCF partial geometry optimization calculations at the *R*(C−F) values of 3.5 and 4.0 Å. The energy value at *R*(C−F) = 4.0 Å given in Table 3 (as the energy of the $2^2A''$ asymptote product) is the CASPT2 energy calculated at a geometry in which the *R*(C−F) value was equal to 4.0 Å and the other geometric parameter values were set to be equal to those in the CASSCF partially optimized geometry at *R*(C−F) = 3.0 Å. On the basis of the CASPT2//CASSCF relative energy values given in Figure 2, the $2^2A''$ asymptote product is higher in energy than the $1^2A''$ asymptote product by 3.59 eV, which is close to the CASPT2//CASSCF T_0 value of 3.56 eV for the $1^3A''$ state of the CH_3^+ ion. The geometry of the CH_3 fragment in the $2^2A''$ asymptote product (in the CASSCF partially optimized geometry at *R*(C−F) = 3.0 Å) is quite similar to the CASSCF geometry of the $1^3A''$ state of the CH_3^+ ion (see Tables 3 and 4). We conclude that the $2^2A''$ state of the CH_3F^+ ion correlates with the $1^3A''$ state of the CH_3^+ ion.

As shown in Figure 2, the F-loss PECs of the $3^2A'$ and $2^2A''$ states (the two Jahn−Teller component states of B^2E) do not coincide. On the basis of the CASPT2//CASSCF relative energy values given in Figure 2, the $3^2A'$ asymptote product is higher in energy than the $1^2A''$ asymptote product by 3.88 eV, which is close to the CASPT2//CASSCF T_0 value of 3.86 eV for the $1^3A'$ state of the CH_3^+ ion. As shown in Tables 3 and 4, the geometry of the CH_3 fragment in the $3^2A'$ asymptote product is almost identical to the CASSCF geometry of the $1^3A'$ state of the CH_3^+ ion. We conclude that the $3^2A'$ state of the CH_3F^+ ion correlates with the $1^3A'$ state of the CH_3^+ ion. In our previous CASPT2//CASSCF study on the CH_3Cl^+ ion,[12] we failed to calculate the $3^2A'$ Cl-loss PEC.

Along the $1^2A''$, $1^2A'$, $2^2A''$, and $3^2A'$ F-loss PECs the energies increase monotonically with the *R*(C−F) value. The CASPT2//CASSCF energy difference between the asymptote product and the reactant for each of the four states is considered as the predicted dissociation energy (D_e). The CASPT2//CASSCF D_e's are evaluated (using the relative energy values given in Figure 2) to be 1.89 eV for the CH_3F^+ ($1^2A''$) → CH_3^+ ($1^1A_1'$) + F dissociation, 1.78 eV for the CH_3F^+ ($1^2A'$) → CH_3^+ ($1^1A_1'$) + F dissociation, 1.81 eV for the CH_3F^+ ($2^2A''$) → CH_3^+ ($1^3A''$) + F dissociation, and 2.06 eV for the CH_3F^+ ($3^2A'$) → CH_3^+ ($1^3A_1'$) + F dissociation. We assume that AP for CH_3^+ ($1^1A_1'$) [AP for production of the CH_3^+ ($1^1A_1'$) ion from the ground-state CH_3F molecule] be equal to the sum of the experimental AIP value of 12.533 eV for the X^2E state[21] and the CASPT2//CASSCF D_e value of 1.89 eV for F-loss dissociation from the $1^2A''$ ground state of CH_3F^+, and the predicted AP value of 14.42 eV for CH_3^+ ($1^1A_1'$) is close to the experimental values of 14.51 eV,[3] 14.55 eV,[2] and 14.71 eV (evaluated by Olney et al.[7] using experimental thermodynamic data). We assume that APs for CH_3^+($1^3A''$) and CH_3^+($1^3A'$) be equal to the sums of the value of 12.533 eV and the CASPT2//CASSCF relative energy values (to the $1^2A''$ reactant) of the $2^2A''$ and $3^2A'$ asymptote products, respectively, and the predicted AP values are 18.01 and 18.30 eV for CH_3^+($1^3A''$) and CH_3^+($1^3A'$), respectively.

For the $2^2A'$ repulsive state, we calculated the CASPT2//CASSCF F-loss PEC starting at an *R*(C−F) value of 1.4 Å. Along the $2^2A'$ F-loss PEC the energy decreases almost monotonically with the *R*(C−F) value. We say "almost" because the energies at the *R*(C−F) values of 2.0 and 2.6 Å are slightly higher than those at the *R*(C−F) values of 1.8 and 2.3 Å, respectively (see Table 3).

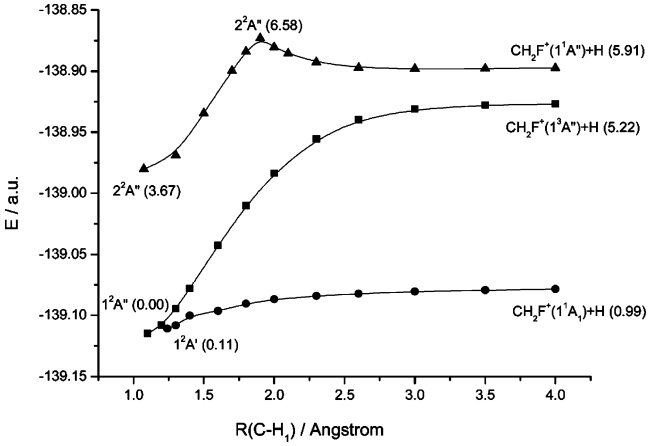

Figure 3. CASPT2//CASSCF potential energy curves for H-loss dissociation from the $1^2A''$, $1^2A'$, and $2^2A''$ states. In parentheses are given the CASPT2//CASSCF relative energies (in eV) of the asymptote products to the $1^2A''$ reactant.

III.C. H-Loss Dissociation. In Figure 3 are given the CASPT2//CASSCF H-loss PECs of the $1^2A''$, $1^2A'$, and $2^2A''$ states of the CH_3F^+ ion. The CH_3F^+ systems in the three states at the $R(C-H_1)$ value of 4.0 Å will be called H-loss asymptote products of the three states in the present section. The CASPT2//CASSCF relative energies of the asymptote products of the three states to the $1^2A''$ reactant are given in parentheses in Figure 3. In Table 5 are listed the CASPT2//CASSCF energies of the three states at selected $R(C-H_1)$ values, together with charges on the H_1 atom [$Q(H_1)$] and values of principal geometric parameters in the CASSCF partially optimized geometries. We failed to calculate the $3^2A'$ H-loss PEC due to convergence problems in the CASSCF partial geometry optimization calculations. The calculations for exploring H-loss dissociation from the $2^2A'$ state will be mentioned at the end of the present section.

As shown in Table 5, the $Q(H_1)$ values in the $1^2A''$, $1^2A'$, and $2^2A''$ asymptote products are all small (≤ 0.010 *e*), which indicates that the products of H-loss dissociation from the three states are the neutral H atom plus the CH_2F^+ ion in different states. In Table 6 are given the CASSCF geometries and CASPT2//CASSCF relative energies (T_0's) for the $1^1A'$ (1^1A_1), $1^3A''$, and $1^1A''$ states (the three lowest-lying states) of the CH_2F^+ ion. As shown in Figure 3, the H-loss PECs of the $1^2A''$ and $1^2A'$ states (the two Jahn−Teller component states of X^2E) of the CH_3F^+ ion do not coincide, and the $1^2A'$ PEC lies below the $1^2A''$ (X^2A'') PEC. As shown in Tables 5 and 6, the geometry of the CH_2F fragment in the $1^2A'$ asymptote product is almost identical to the CASSCF geometry of the 1^1A_1 state of the CH_2F^+ ion. We conclude that the $1^2A'$ state of the CH_3F^+ ion correlates with the 1^1A_1 (ground) state of the CH_2F^+ ion. On the basis of the CASPT2//CASSCF relative energy values given in Figure 3, the $1^2A''$ asymptote product is higher in energy than the $1^2A'$ asymptote product by 4.23 eV, which is close to the CASPT2//CASSCF T_0 value of 4.17 eV for the $1^3A''$ state of the CH_2F^+ ion. As shown in Tables 5 and 6, the geometry of the CH_2F fragment in the $1^2A''$ asymptote product is almost identical to the CASSCF geometry of the $1^3A''$ state of the CH_2F^+ ion. We conclude that the $1^2A''$ (ground) state of the CH_3F^+ ion correlates with the $1^3A''$ (excited) state of the CH_2F^+ ion.

On the basis of the CASPT2//CASSCF relative energy values given in Figure 3, the $2^2A''$ asymptote product is higher in energy than the $1^2A'$ asymptote product by 4.92 eV, which is close to the CASPT2//CASSCF T_0 value of 4.96 eV for the $1^1A''$ state of the CH_2F^+ ion. As shown in Tables 5 and 6, the geometry of the CH_2F fragment in the $2^2A''$ asymptote product is almost identical to the CASSCF geometry of the $1^1A''$ state of the CH_2F^+ ion. We conclude that the $2^2A''$ state of the CH_3F^+ ion correlates with the $1^1A''$ state of the CH_2F^+ ion.

Along the $1^2A'$ and $1^2A''$ H-loss PECs the energies increase monotonically with the $R(C-H_1)$ value. The CASPT2//CASSCF D_e's are evaluated (using the relative energy values given in Figure 3) to be 0.88 eV for the CH_3F^+ ($1^2A'$) → CH_2F^+ (1^1A_1) + H dissociation and 5.22 eV for the CH_3F^+ ($1^2A''$) → CH_2F^+ ($1^3A''$) + H dissociation. By adding the experimental AIP value of 12.533 eV (see above) and the CASPT2//CASSCF relative energy values (to the $1^2A''$ reactant) of the $1^2A'$ and $1^2A''$ asymptote products, the AP value for CH_2F^+ (1^1A_1) is evaluated to be 13.52 eV, which is quite close to the experimental values of 13.2 eV,[2] 13.50 eV,[4] 13.37 eV,[6] and 13.45 eV (evaluated by Olney et al.[7] using experimental thermodynamic data), and the AP value for CH_2F^+ ($1^3A''$) is evaluated to be 17.75 eV.

As shown in Figure 3, there exists an energy maximum at an $R(C-H_1)$ value of 1.9 Å along the $2^2A''$ PEC, which indicates

TABLE 5: CASPT2//CASSCF Energies (*E*'s) at the Selected $R(C-H_1)$ Values for H-Loss Dissociation in the $1^2A''$, $1^2A'$, and $2^2A''$ States, Together with Charge Values (*Q*'s) on the Departing H_1 Atom and Values of Principal Geometric Parameters in the CASSCF Partially Optimized Geometries[a]

R(C-H_1) (Å)	E (au)	$Q(H_1)$ (*e*)	R(C−F) (Å)	$A(H_2CF)$ (deg)	$D(H_2CFH_2')$ (deg)
		$1^2A''$			
1.096	−139.11499	0.367	1.280	112.4	76.1
1.2	−139.10798	0.250	1.278	112.6	76.8
1.4	−139.07805	0.128	1.274	113.2	78.5
1.6	−139.04274	0.105	1.270	113.9	80.3
1.8	−139.01027	0.113	1.266	114.6	82.2
2.0	−138.98359	0.117	1.263	115.4	84.1
2.3	−138.95552	0.095	1.258	116.5	87.0
2.6	−138.93989	0.060	1.254	117.4	88.9
3.0	−138.93110	0.029	1.252	117.8	90.0
4.0	−138.92683	0.005	1.251	118.0	90.8
		$1^2A'$			
1.237	−139.11086	0.337	1.301	114.7	153.4
1.4	−139.10029	0.182	1.267	116.1	159.8
1.6	−139.09641	0.146	1.261	116.5	162.6
1.8	−139.09054	0.093	1.250	117.0	168.0
2.0	−139.08687	0.062	1.242	117.2	172.3
2.3	−139.08406	0.040	1.236	117.3	176.5
2.6	−139.08227	0.031	1.234	117.3	178.4
3.0	−139.08060	0.022	1.233	117.3	179.6
4.0	−139.07860	0.006	1.232	117.3	180.0
		$2^2A''$			
1.073	−138.98015	0.390	1.623	107.2	100.8
1.3	−138.96904	0.180	1.612	109.8	96.3
1.5	−138.93445	0.122	1.609	110.0	97.5
1.7	−138.89971	0.126	1.603	110.7	99.2
1.8	−138.88403	0.132	1.599	110.9	100.0
1.9	−138.87301	−0.056	1.252	116.5	96.7
2.0	−138.88036	−0.041	1.251	116.6	97.4
2.3	−138.89289	0.007	1.252	117.0	99.0
2.6	−138.89726	0.010	1.253	117.1	99.9
3.0	−138.89815	0.013	1.253	117.2	100.3
4.0	−138.89792	0.010	1.253	117.3	100.5

[a] For notations, see Figure 1.

TABLE 6: CASSCF Geometries and CASPT2//CASSCF Relative Energies (T_0's) for the 1^1A_1, $1^3A''$, and $1^1A''$ States (the Three Lowest-Lying States) of the CH_2F^+ Ion

state	R(C−H) (Å)	R(C−F) (Å)	A(HCF) (deg)	D(HCFH′) (deg)	T_0 (eV)
1^1A_1	1.089	1.232	116.9	180.0	0.00
$1^3A''$	1.177	1.251	118.0	90.7	4.17
$1^1A''$	1.172	1.253	117.3	100.5	4.96

TABLE 7: CASPT2//CASSCF Dissociation Energies (D_e's) for F-Loss and H-Loss from the $1^2A''$, $1^2A'$, $2^2A'$, $2^2A''$, and $3^2A'$ States of the CH_3F^+ Ion and CASPT2//CASSCF Appearance Potentials (APs) for the Production of the CH_3^+ and CH_2F^+ Ions in Their Ground and Excited States from CH_3F

	F-loss dissociation			H-loss dissociation		
CH_3F^+	product (+F)	D_e (eV)	AP (eV)	product (+H)	D_e (eV)	AP (eV)
$1^2A''$	CH_3^+ ($1^1A_1'$)	1.89	14.42[a] (exptl 14.55[b], 14.51[c], 14.71[d])	CH_2F^+ ($1^3A''$)	5.22	17.75[a]
$1^2A'$	CH_3^+ ($1^1A_1'$)	1.78	14.42[a]	CH_2F^+ (1^1A_1)	0.88	13.41[a] (exptl 13.2[c], 13.5[e], 13.45[d])
$2^2A'$	CH_3^+ ($1^1A_1'$)	f		g		
$2^2A''$	CH_3^+ ($1^3A''$)	1.81	18.01[a]	CH_2F^+ ($1^1A''$)	2.91[h]	18.17[i]
$3^2A'$	CH_3^+ ($1^3A'$)	2.06	18.30[a]	j		

[a] Evaluated as the sums of the experimental AIP value of 12.533 eV for the X^2E state (given in ref 21) and the CASPT2//CASSCF relative energies for the dissociation asymptote products to the $1^2A''$ reactant (the $1^2A''$ state at the CASSCF equilibrium geometry). [b] From ref 2. [c] From ref 3. [d] Evaluated by Olney et al. (see ref 7) using experimental thermodynamic data. [e] From ref 4. [f] The $2^2A'$ state is repulsive about the C−F bond. [g] The calculated $2^2A'$ PEC did not lead to $H + CH_2F^+$, but to $H^+ + CH_2F$. [h] CASPT2//CASSCF relative energy of the barrier (see text) to the $2^2A''$ reactant. [i] Evaluated as the sum of the experimental AIP value of 12.533 eV for the X^2E state (given in ref 21) and the CASPT2//CASSCF relative energy of the barrier to the $1^2A''$ reactant. [j] The $3^2A'$ H-loss PEC calculations were not successful.

an energy barrier in the CH_3F^+ ($2^2A''$) → CH_2F^+ ($1^1A''$) + H dissociation reaction. At the CASPT2//CASSCF level the $2^2A''$ maximum is predicted to be 6.58 eV higher in energy than the $1^2A''$ reactant and to be 2.91 and 0.67 eV higher than the $2^2A''$ reactant and asymptote product, respectively. We assume that AP for CH_2F^+ ($1^1A''$) be equal to the sum of the experimental AIP value of 12.533 eV (see above) and the CASPT2//CASSCF relative energy value (to the $1^2A''$ reactant) of the $2^2A''$ maximum, and the AP value is evaluated to be 19.11 eV. We note that the dominant configuration in the CASSCF wave function of the $2^2A''$ state is $...(5a')^2(1a'')^1(6a')^2(7a')^2(2a'')^2$ at small $R(C-H_1)$ values and it is $...(5a')^2(1a'')^2(6a')^2(7a')^1(2a'')^1(8a')^1$ at large $R(C-H_1)$ values. The $2^2A''$ maximum is considered as an indication of a potential energy surface avoided-crossing between two $^2A''$ states, one representing a primary ionized state $[(1a'')^{-1}]$ and the other a shake-up ionized state $[(7a')^{-1}(2a'')^{-1}(8a')^1]$. It is noted in Table 5 that variances of the $Q(H_1)$ and $R(C-F)$ values between $R(C-H_1) = 1.8$ Å and $R(C-H_1) = 1.9$ Å are quite large.

The experimental workers[1] did not observe H-loss dissociation from the A ($2^2A'$) state of the CH_3F^+ ion. We tried to calculate a $2^2A'$ H-loss PEC, and the CASPT2//CASSCF calculations were performed at selected $R(C-H_1)$ values ranging from 1.2 to 4.0 Å. Along the calculated $2^2A'$ PEC the energy varies continuously with the $R(C-H_1)$ value, and an energy maximum exists at $R(C-H_1)$ value of 1.7 Å (the CASSCF wave functions have different dominant configurations at the $R(C-H_1)$ values smaller and larger than 1.7 Å). However, the $Q(H_1)$ value of +0.998 *e* at $R(C-H_1) = 4.0$ Å indicates that this $2^2A'$ PEC would lead to the dissociation product of $H^+ + CH_2F$. The CASPT2//CASSCF energy value (−138.90765 au) of the $2^2A'$ state of CH_3F^+ at $R(C-H_1) = 4.0$ Å is close to the CASPT2//CASSCF energy value (−138.90456 au) of the $1^2A'$ ground state of the CH_2F radical. These preliminary results imply that H-loss dissociation does not occur from the $2^2A'$ state but a proton loss (deprotonation) process may occur.

IV. Conclusions

The $1^2A''$, $1^2A'$, $2^2A'$, $2^2A''$, and $3^2A'$ states of the CH_3F^+ ion have been studied by using the CASSCF and CASPT2 methods. The $1^2A''$ state, one of the two Jahn−Teller component states of X^2E, is predicted to be the ground state, and the $2^2A'$ (A^2A_1) state is predicted to be repulsive. The CASPT2//CASSCF T_0 values for $2^2A''$ and $3^2A'$ (the two Jahn−Teller component states of B^2E) are very close to the experimental T_0 value for the B state. The CASPT2 T_v' values for $2^2A'$, $2^2A''$, and $3^2A'$ are in reasonable agreement with the experimental T_v' values for the A and B states.

At the CASPT2//CASSCF level we calculated F-loss dissociation PECs of the five C_s states and H-loss dissociation PECs of the $1^2A''$, $1^2A'$, and $2^2A''$ states. In Table 7 we collect the calculated D_e's for the F-loss and H-loss dissociation reactions and the evaluated APs for the CH_3^+ and CH_2F^+ ions in different states. On the basis of these calculation results, we present our comments on the general picture (see Introduction) of Eland et al. for dissociation of the CH_3F^+ ion from the X, A, and B states. The calculations indicate that F-loss dissociation occurs from the $1^2A''$, $1^2A'$, and $2^2A'$ states, which supports the observations of direct dissociation from the X and A states by Eland et al., and that the produced CH_3^+ ions are all in the $1^1A_1'$ ground state. The calculations indicate that H-loss dissociation occurs from the $1^2A''$, $1^2A'$, and $2^2A''$ states, which supports the observations of direct dissociation from the X and B states by Eland et al., and that the produced CH_2F^+ ions are in the $1^3A''$, 1^1A_1 (the ground state), and $1^1A''$ states, respectively. The calculations indicate that direct F-loss dissociation occurs from the $2^2A''$ and $3^2A'$ states (the two Jahn−Teller component states of B^2E) and the produced CH_3^+ ions are in the $1^3A''$ and $1^3A'$ states, respectively. In the H-loss PEC calculations for $2^2A'$, the H^+ ion was found to be the dissociation product. Our calculations clearly show that the H-loss PECs of the two Jahn−Teller component states ($1^2A'$ and $1^2A''$) of X^2E converge to the different dissociation limits and that the F-loss PECs of the two Jahn−Teller component states ($3^2A'$ and $2^2A''$) of B^2E converge to the different dissociation limits.

We previously studied the X^2E ($1^2A'$, $1^2A''$), A^2A_1 ($2^2A'$), and B^2E ($3^2A'$, $2^2A''$) states of the CH_3Cl^+ ion[12] using the same methods (the calculations for $3^2A'$ of CH_3Cl^+ were not successful). We will compare the predicted properties and dissociation mechanisms for the CH_3Cl^+ and CH_3F^+ ions. The Jahn−Teller splitting patterns in the X^2E states of the CH_3Cl^+ and CH_3F^+ ions are different: the ground state being $1^2A''$ for CH_3F^+ while $1^2A'$ for CH_3Cl^+. The $2^2A'$, $2^2A''$, and $3^2A'$ states of CH_3F^+ are very close in energy at the CH_3F molecular geometry, while the energy gap between the $2^2A'$ and $2^2A''$ states of CH_3Cl^+ is larger than 1 eV at the CH_3Cl molecular geometry.

The CASPT2//CASSCF calculations indicate that the $1^2A''$, $1^2A'$, $2^2A'$, and $2^2A''$ Cl-loss PECs of CH_3Cl^+ have the same general features as the $1^2A''$, $1^2A'$, $2^2A'$, and $2^2A''$ F-loss PECs

of CH_3F^+, respectively, and that the $1^2A'$, $1^2A''$, and $2^2A'$ states of CH_3Cl^+ and CH_3F^+ correlate with the $1^1A_1'$ state of CH_3^+ and the $2^2A''$ states of CH_3Cl^+ and CH_3F^+ correlate with the $1^3A''$ state of CH_3^+. Though the Cl-loss PEC calculations for the $3^2A'$ state of CH_3Cl^+ were not successful, we would assume that the $3^2A'$ state of CH_3Cl^+ would correlate with the $1^3A'$ state of CH_3^+ as the $3^2A'$ state of CH_3F^+. The Cl-loss asymptote product for $3^2A'$ would be higher in energy than that for $2^2A''$ based on this assumption, while the starting point (the energy of the equilibrium geometry) of the $3^2A'$ Cl-loss PEC would be lower in energy than that of the $2^2A''$ Cl-loss PEC if the Jahn−Teller splitting pattern in B^2E of CH_3Cl^+ is the same as that in X^2E of CH_3Cl^+.

The CASPT2//CASSCF calculations indicate that the $1^2A'$, $1^2A''$, and $2^2A''$ H-loss PECs of CH_3Cl^+ have the same general features as the $1^2A'$, $1^2A''$, and $2^2A''$ H-loss PECs of CH_3F^+, respectively, and that the $1^2A'$, $1^2A''$, and $2^2A''$ states of both the ions correlate with the 1^1A_1, $1^3A''$, and $1^1A''$ states of CH_2X^+ (X = Cl or F), respectively. The $1^2A''$ ground state of CH_3F^+ correlates with the $1^3A''$ excited state of CH_2F^+. The $3^2A'$ H-loss PEC calculations were not successful for either CH_3Cl^+ or CH_3F^+. For exploring H-loss dissociation from the $2^2A'$ states of CH_3Cl^+ and CH_3F^+, the CASPT2//CASSCF E [R(C−H_1)] PECs were calculated, but the calculated PECs did not lead to $H + CH_2X^+$. The calculated $2^2A'$ PEC of CH_3Cl^+ led to CH_2ClH^+ (H-migration process), while the calculated $2^2A'$ PEC of CH_3F^+ led to $H^+ + CH_2F$.

Acknowledgment. This work was supported by the National Natural Science Foundation Committee of China (No. 20333050).

References and Notes

(1) Eland, J. H. D.; Frey, R.; Kuestler, A.; Schulte, H.; Brehm, B. *Int. J. Mass Spectrom. Ion Phys.* **1976**, *22*, 155.

(2) Locht, R.; Momigny, J. *Chem. Phys.* **1996**, *206*, 225.

(3) Weitzel, K.-M.; Güthe, F.; Mähnert, J.; Locht, R.; Baumgärtel, H. *Chem. Phys.* **1995**, *201*, 287.

(4) Locht, R.; Momigny, J.; Rühl, E.; Baumgartel, H. *Chem. Phys.* **1987**, *117*, 305.

(5) Locht, R.; Momigny, J. *Int. J. Mass Spectrom. Ion Processes* **1986**, *71*, 141.

(6) Momigny, J.; Locht, R.; Caprace, G. *Int. J. Mass Spectrom. Ion Processes* **1986**, *71*, 159.

(7) Olney, T. N.; Cooper, G.; Chan, W. F.; Burton, G. R.; Brion, C. E.; Tan, K. H. *Chem. Phys.* **1994**, *189*, 733.

(8) Lossing, F. P. *Bull. Soc. Chim. Belg.* **1972**, *81*, 125.

(9) Roos, B. O. In *Ab Initio Methods in Quantum Chemistry*; Lawley, K. P., Ed.; Wiley: New York, 1987; Part 2.

(10) Andersson, K.; Malmqvist, P.-Å.; Roos, B. O.; Sadley, A. J.; Wolinski, K. *J. Phys. Chem.* **1990**, *94*, 5483.

(11) Andersson, K.; Malmqvist, P.-Å.; Roos, B. O. *J. Chem. Phys.* **1992**, *96*, 1218.

(12) Xi, H.-W.; Huang, M.-B.; Chen, B.-Zh.; Li, W.-Z. *J. Phys. Chem. A* **2005**, *109*, 4381.

(13) Locht, R.; Leyh, B.; Hoxha, A.; Dehareng, D.; Jochims, H. W.; Baumgärtel, H. *Chem. Phys.* **2000**, *257*, 283.

(14) Mahapatra, S.; Vallet, V.; Woywod, C.; Köppel, H.; Domcke, W. *Chem. Phys.* **2004**, *304*, 17.

(15) Gauld, J. W.; Radom, L. *J. Phys. Chem.* **1994**, *98*, 777.

(16) Andersson, K.; Fulscher, M. P.; Lindh, R.; Malmqvist, P.-Å.; Olsen, J.; Sadlej, A. J.; Widmark, P.-O. *MOLCAS*, version 5.4; University of Lund: Sweden, 2002.

(17) Almlöf, J.; Taylor, P. R. *J. Chem. Phys.* **1987**, *86*, 4070.

(18) Widmark, P.-O.; Malmqvist, P.-Å.; Roos, B. O. *Theor. Chim. Acta* **1990**, *77*, 291.

(19) Widmark, P.-O.; Persson, B.-J.; Roos, B. O. *Theor. Chim. Acta* **1990**, *79*, 419.

(20) Demaison, J.; Breidung, J.; Thiel, W.; Papousek, D. *Struct. Chem.* **1999**, *10*, 129.

(21) Karlsson, K.; Jadrny, R.; Mattsson, L.; Chau, F. T.; Siegbahn, K. *Phys. Scr.* **1977**, *16*, 225.